

Spin Spring Behavior in Exchange Coupled Soft and High-Coercivity Hard Ferromagnets

R.D. Shull,¹ A.J. Shapiro,¹ V.S. Gornakov,^{1,2} V.I. Nikitenko,^{1,2} J. Samuel Jiang,³ H. Kaper,³
G. Leaf,³ and S.D. Bader³

¹*National Institute of Standards and Technology, Gaithersburg, MD 20899*

²*Institute of Solid State Physics, Russian Academy of Sciences, Chernogolovka 142432 Russia*

³*Materials Science Division, Argonne National Laboratory, Argonne, IL 60439*

The submitted manuscript has been created by the University of Chicago as Operator of Argonne National Laboratory ("Argonne") under Contract No. W-31-109-ENG-38 with the U.S. Department of Energy. The U.S. Government retains for itself, and others acting on its behalf, a paid-up, nonexclusive, irrevocable worldwide license in said article to reproduce, prepare derivative works, distribute copies to the public, and perform publicly and display publicly, by or on behalf of the Government.

Paper submitted for the Proceedings of the 8th Joint Magnetism and Magnetic Materials-INTERMAG Conference, San Antonio, TX, Jan. 7-11, 2001, to be published by IEEE Trans. Mag.

DISCLAIMER

This report was prepared as an account of work sponsored by an agency of the United States Government. Neither the United States Government nor any agency thereof, nor any of their employees, make any warranty, express or implied, or assumes any legal liability or responsibility for the accuracy, completeness, or usefulness of any information, apparatus, product, or process disclosed, or represents that its use would not infringe privately owned rights. Reference herein to any specific commercial product, process, or service by trade name, trademark, manufacturer, or otherwise does not necessarily constitute or imply its endorsement, recommendation, or favoring by the United States Government or any agency thereof. The views and opinions of authors expressed herein do not necessarily state or reflect those of the United States Government or any agency thereof.

DISCLAIMER

Portions of this document may be illegible in electronic image products. Images are produced from the best available original document.

Spin spring behavior in exchange coupled soft and high-coercivity hard ferromagnets.

R.D. Shull¹, A.J. Shapiro¹, V.S. Gornakov^{1,2}, V.I. Nikitenko^{1,2}, J. Samuel Jiang³, H. Kaper³, G. Leaf³, and S.D. Bader³.

¹National Institute of Standards and Technology, Gaithersburg, MD 20899;

²Institute of Solid State Physics, Russian Academy of Sciences, Chernogolovka, 142432 Russia;

³Argonne National Laboratory, Argonne, IL 60439

The magnetization reversal processes in an epitaxial Fe/Sm₂Co₇ structure were investigated using the magneto-optical indicator film technique. The dependence of the magnitude and the orientation of the structure average magnetization have been studied on both cycling and rotating the external magnetic field. It was discovered that the magnetization reversal of the soft ferromagnet can proceed by formation of not only one-dimensional, but also two-dimensional, exchange spin springs. Experimental data is compared with a theoretical estimation of the rotational hysteresis loop for a spin system containing a one-dimensional exchange spring.

Understanding the mechanisms of magnetization reversal is a fundamental issue in magnetism. For coupled magnetic systems, in particular, detailed knowledge of the magnetization reversal processes holds the key to unlocking the potential for applications. For example, in exchange-spring permanent magnets consisting of nanodispersed hard and soft magnetic phases coupled at the interfaces, the magnetization reversal of the soft phase limits the maximum achievable energy product^{1,2}. For antiferromagnet/ferromagnet exchange bias structures³, the strength of the interfacial pinning realized experimentally is significantly reduced from expectation for reasons that have largely alluded researchers.

In this paper, we present a study to visualize the magnetization reversal process in an exchange-spring Fe/Sm-Co bilayer using the magneto-optic indicator film (MOIF) technique. The MOIF technique⁴ is sensitive to stray fields emanating from magnetic structures, such as from domain walls, Bloch's lines, and crystal defects (e.g. dislocations, voids and sample edges). A thin film of yttrium iron garnet (YIG) doped with Bi, having an in-plane magnetization and a large Faraday effect, is used as an indicator of such leakage fields

The exchange-spring film was prepared by d.c. magnetron sputtering onto a Cr-buffered single-crystalline MgO(100) substrate, and has the configuration Fe(500Å)/Sm₂Co₇(350Å). Details of the preparation conditions have been described elsewhere^{5,6}. The epitaxial growth of the Sm-Co layer gives rise to an in-plane four-fold magnetic anisotropy and a high coercivity⁶. The magnetically soft Fe layer is exchange coupled to the Sm-Co hard magnet layer. Once saturated, the Sm-Co layer remains magnetized along an easy direction.

For MOIF imaging, a hole was bored through the bilayer sample, and then the YIG film was placed directly on the sample surface. Around the edge of the hole, the normal component of the leakage field locally causes the magnetization of the indicator film to deviate from its initially in-plane orientation. This deviation induces a Faraday rotation in a polarized light beam, giving rise to black and white optical contrast. The location and intensity of the bright and dark areas around the hole are determined by the direction and magnitude of the leakage

field and provide a means for estimating the average magnetization *M*. For this bilayer, the total magnetic moment in the Fe layer is far greater than that in the Sm-Co layer. The magneto-optical (MO) contrast is therefore dominated by the magnetization behavior of the Fe layer.

A set of MOIF images in fig.1, shows the remagnetization process of the Fe layer, when the reverse field is precisely aligned with the unidirectional anisotropy axis. In this case, the magnetization reversal process proceeds non-uniformly as there is no preferred chirality to initiate the uniform rotation process. The average magnetization direction remains collinear with the field direction, but there is a change in MO contrast during the reversal (Fig.2). For application of reversal fields > μ₀H_{cr} (≅ 10 mT), where H_{cr} is some critical field, the MO intensity does not change significantly. However, for reversal fields less than this critical value, the MO image contrast decreases with increasing field amplitude. Initially the contrast decreases slowly (Fig.1b, 2), and then more rapidly with increased |H|. The MO contrast disappears completely at H ≈ -50 mT (Fig.1c) and reappears with opposite sign at fields greater than -80 mT (Fig.1d). For magnetic fields in excess of -100 mT, the MO contrast remains constant.

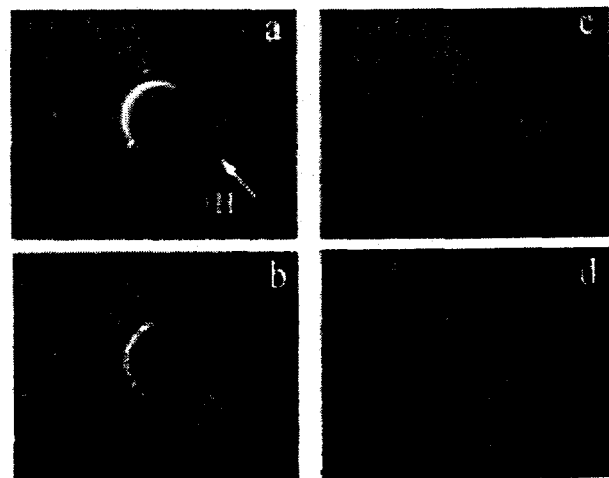


FIG. 1. MO images of the sample region near the hole at reverse field.

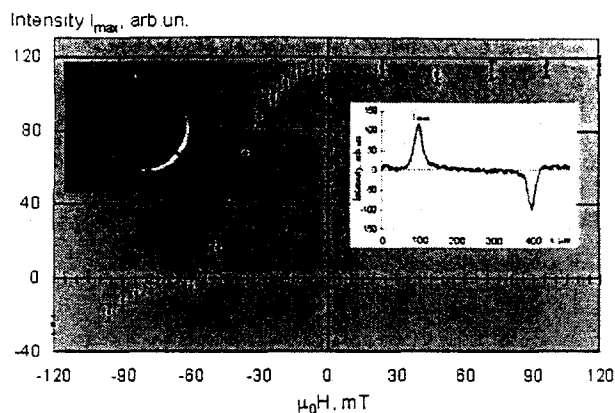
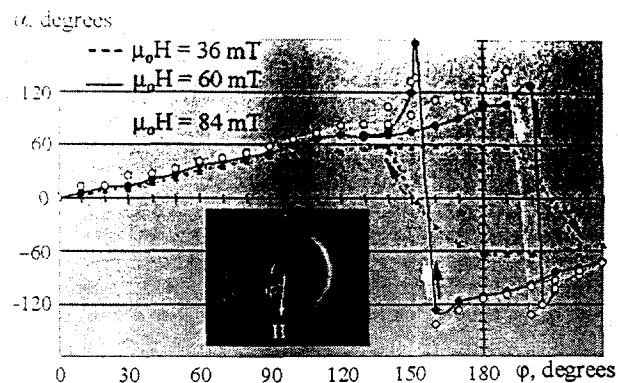


FIG. 2. Maximum intensity (shown on the right inset) of the MO signal (measured along profile line on the left inset) vs. field amplitude during magnetization reversal.

The magnetization reversal mechanism of the soft layer is determined by non-uniform rotation of Fe spins in local microscopic areas. Since the reversal field is aligned with the unidirectional axis, there is no preferred macroscopic direction for spin winding in the Fe layer. However, it is possible that local deviations in magnetic anisotropy axes break the left-right symmetry, and the Fe layer breaks up into two groups of micro-regions wherein the Fe spins rotate in opposite directions. On average, the magnetization components perpendicular to the field direction cancel out, leaving the direction of the M unchanged. But, the increased rotation of the Fe spins reduces the density of poles around the hole and thus the MO contrast decreases.

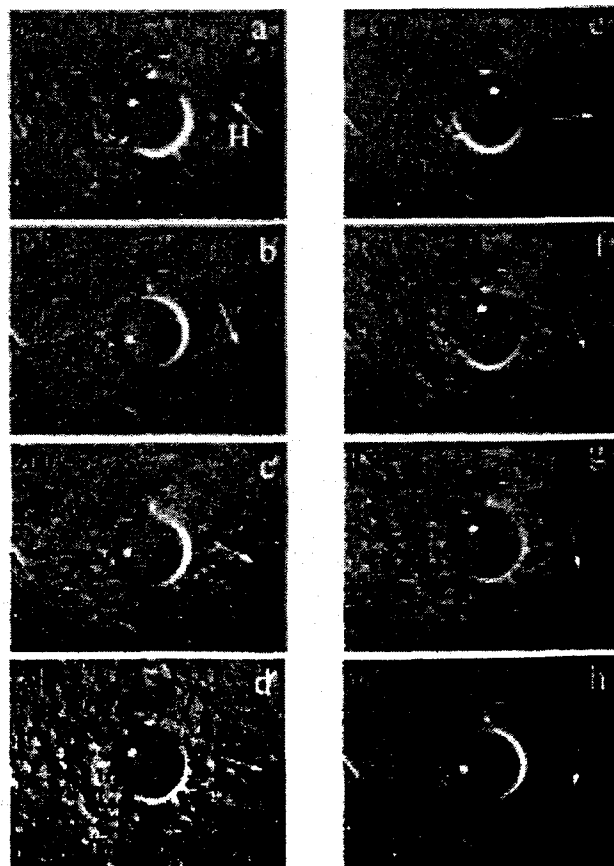
In Fig. 3 a sequence of MOIF images shows the response of the Fe layer when the applied field is fixed in magnitude but is rotated by angle ϕ in the film plane. From the easy magnetization direction (Fig. 3a), as ϕ increases, the magnetization smoothly rotates with the field with some phase delay (Fig. 3b). After the field reaches the critical angle value ϕ_1 , the total magnetization begins to rotate in the opposite direction while the field direction continues to change in the original direction (Fig. 3c,d). The subsequent rotation of the total magnetization, after completion of this stage of inverse rotation (Fig. 3e), is again in synchronization with the field. But in this latter case, as one might expect, M takes the phase lead over H up to the point where they both coincide with the unidirectional anisotropy axis.

Fig. 4 reveals hysteresis in the magnetization rotation. Since the fields available are too small to switch the hard layer, the total magnetization is never reoriented against the unidirectional anisotropy. But we see in Fig. 4 that M jumps to a new equilibrium position symmetrically oriented with respect to the axis of the unidirectional anisotropy after the field reaches the critical angle ϕ_1 . This angle and the broadness of the transitional region depend on the field magnitude, with a broader transitional region being observed at lower fields. The process associated with the transition into a new position at $\mu_0H = 36$ mT is illustrated in Fig. 3. Rotation of the field direction in the opposite sense (Fig. 3e-h) leads to a magnetization rotation process in the opposite direction



with new critical angle ϕ_2 where $\phi_2 < \phi_1$. This results in a hysteresis in the angular rotation process of the magnetization.

Interestingly a non-uniform MO intensity appears across the sample surface during the inverse rotation of M . This non-uniformity begins to develop in Fig. 3c (or Fig. 3f), and becomes most intense in Fig. 3d (or Fig. 3g) where the effective total magnetization is oriented along the unidirectional anisotropy axis. Finally, the MO signal in the sample again becomes homogeneous (Fig. 3e and 3a). The non-uniform signal is caused by the inhomogeneous distribution of the real magnetization in the plane of the Fe layer.



As Fig. 4 shows, upon the initial rotation of H , M

FIG. 3. MO images of the sample region near the hole during in-plane field rotation for $\mu_0H = 36$ mT. The white and black arrow indicates the directions of H and M

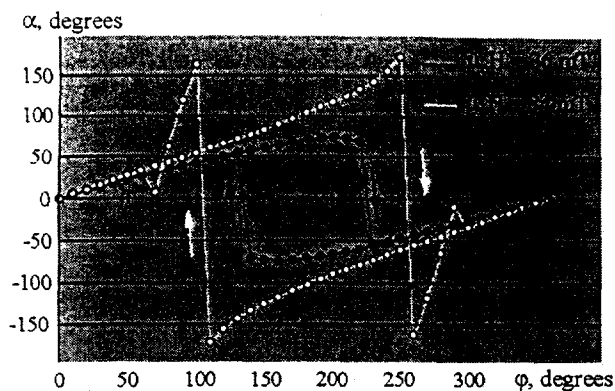


FIG. 5. Rotation angle of M (α) vs. the magnetic field rotation angle (ϕ) for different field amplitude calculated from the one-dimensional model.

MEASUREMENTS.

follows the field, although with some delay. At larger field rotation angles ϕ , larger magnetization jumps take place in a narrower range of the angle α , and the character of the inverse rotation is less easily discerned. With increased field magnitudes, the rotational hysteresis loops possess not only sharper M transitions as previously noted, but also the appearance of abnormal peaks "before" and "after" the two discontinuous jumps in angle α .

Using a one-dimensional rotation model, we calculated the ϕ -dependence of the magnetization direction (α) at two H values (shown in Fig. 5). There is obviously good qualitative agreement with the experimental data of Fig. 4. The calculated results possess the same rotational hysteresis loop, a phase delay of M with increasing ϕ , and the surprising peaks before and after the two discontinuous jumps in angle α in higher H magnitude. This similarity in computation and experiment confirms the suggestion that M loses stability after the field reaches some critical angle.

However, there is a marked quantitative disagreement in the loop broadness between the calculated and experimental data. The measured loops are narrower and less sharp than calculated ones. Also, in the calculated case, the critical angles increase with increasing H magnitude instead the experimentally observed decrease in ϕ_1 and ϕ_2 .

The one-dimensional model indicates a rotational instability of the exchange springs, but cannot give the correct critical ϕ magnitudes because it doesn't take into account the more complete non-linear processes of nucleation and motion of nanodomains. The MOIF visualization technique, however, has revealed new information regarding the structural and kinetic details of the remagnetization process in bilayers with coupled magnetically soft and hard exchange layers.

In an earlier paper of ours, MOIF imaging of the remagnetization process with the reversal field offset from the easy magnetization axis⁶ revealed that a magnetization rotation of the magnetically soft layer was present. Nevertheless, the remagnetization process when the reversal field is exactly aligned with the easy

magnetization axis is quite inhomogeneous. As a first approximation, one can assume that the MO intensity at the hole edges corresponds to the average magnetization M along the full thickness of the bilayer. Under this assumption, the vanishing MO contrast in Fig. 1c and the appearance of a reversed contrast in Fig. 1d do not contradict the systematics observed in Fig. 3. For $\phi = 0$, the spins rotate in opposite directions in different micro areas similar to that of the experimental conditions in Fig. 3c and Fig. 3f. This locally inhomogeneous rotation results initially in the complete compensation (Fig. 1c) and subsequently in the development of the opposite polarity for the total magnetization.

This conclusion is confirmed by the rotational

hysteresis experiments presented in Figs. 3, 4. During smooth rotation of a sufficiently strong field, the spins of all micro areas in the Fe film plane rotate in the same direction. That leads to a M rotation without substantial weakening of the MO contrast, which is determined mainly by the thick Fe layer since it has a substantially higher saturation magnetization, M_s , than does the Sm-Co layer.

The most vivid display of the non-uniform spin rotation in the Fe-layer is the appearance of the "ripple structure" and domains in Figs. 3c, d, f, g and also in the hysteretic behavior of the angular dependences shown in Fig. 4. The nonlinear dependence of $\alpha(\phi)$ in Fig. 4 also suggests a non-uniform distribution of M_s . Crystal lattice defects in the bilayer and imperfections at the interface must apparently play an important role here.

¹ E. F. Kneller and R. Hawig, *IEEE Trans. Mag.* **27**, 3588 (1991).

² E. E. Fullerton, J. S. Jiang, M. Grimsditch, C. H. Sowers, and S. D. Bader, *Phys. Rev. B* **58**, 12193 (1998).

³ J. Nogués and I. K. Schuler, *J. Magn. Magn. Mater.* **192**, 203 (1999).

⁴ L. H. Bennett, R. D. McMichael, L. J. Swartzendruber, S. Hua, D. S. Lashmore, A. J. Shapiro, V. S. Gornakov, L. M. Dedukh, V. I. Nikitenko, *Appl. Phys. Lett.* **66**, 888 (1995).

⁵ E. E. Fullerton, J. S. Jiang, Christine Rehm, C. H. Sowers, S. D. Bader, J. B. Patel, and X. Z. Wu, *Appl. Phys. Lett.* **71**, 1579 (1997).

⁶ J. S. Jiang, E. E. Fullerton, C. H. Sowers, A. Inomata, S. D. Bader, A. J. Shapiro, R. D. Shull, V. S. Gornakov, and V. I. Nikitenko, *IEEE Trans. Magn.* **35**, 3229 (1999)